ISSN:3139-1192(Online)

SCINTIA

Online Peer-reviewed Multidisciplinary Journal

December 2024
Volume- 2

Netaji Satabarshiki Mahavidyalaya, Ashoknagar,
North 24 Parganas, West Bengal- 743223

Contents lists available at https://scintia.in/

SCINTIA

Online Peer-reviewed Multidisciplinary Journal

ISSN: 3139-1192 (Online)

[Published by Netaji Satabarshiki Mahavidyalaya]

From Degradation to Regeneration: A Remote Sensing-Based Assessment of Cyclone Aila's Impact on Sundarban Mangrove

Dipanjan Das Majumdar

Assistant Professor, Department of Geography, Netaji Satabarshiki Mahavidyalaya, Ashoknagar, West Bengal, India

Abstract

Tropical cyclones pose significant threats to coastal mangrove ecosystems, yet quantitative assessments of their impact on forest canopy structure remain limited. The present study offers the application of Forest Canopy Density (FCD) modelling to evaluate the effects of Cyclone Aila on mangrove ecosystems in Prentice and Lothian islands, Indian Sundarban. LANDSAT 5 TM data for two different time periods (2009 and 2010) were used to evaluate the pre-Aila and post-Aila vegetation conditions. Following radiometric and atmospheric correction, FCD was calculated for 2009 and 2010 using the four complementary spectral indices: AVI, BI, SI, SSI and VD. Model validation employed multiple vegetation indices (NDVI, ANVI, PVI, SAVI, SLAI, COSRI, NDWI) showing strong positive correlations ($r > 0.7$) with FCD outputs. A change detection matrix was derived using class combination analysis between FCD 2009 and FCD 2010 to identify the pixel-to-pixel changes in forest canopy density caused by Aila cyclone. Aila caused extensive canopy degeneration across 14.03 km^2 (27.2 % of the study area) primarily in island interiors where storm surge induced prolonged inundation and hypersaline conditions severely impacted the mangrove vegetation. On the other hand, the study revealed significant ecological resilience and adaptation. Cyclone-induced sedimentation along the rim of the islands facilitated the growth of new mangroves and canopy regeneration. This research demonstrates that

To cite this article: Majumdar, D. D. (2024). From Degradation to Regeneration: A Remote Sensing-Based Assessment of Cyclone Aila's Impact on Sundarban Mangrove. *Scintia*, 2, 59–76.

Cyclone Aila altered ongoing mangrove succession patterns, creating a complex mosaic of degradation and regeneration zones controlled by local geomorphological factors. Thus, it can be concluded that the bio-geomorphic fate of all islands of Sundarban delta system is largely determined by recurrent storm activities. This study establishes the novel application of the FCD model to mangrove forest ecosystems, providing valuable insights for climate change adaptation and mangrove conservation strategies.

Keywords: Forest Canopy Density, Tropical Cyclones, Mangroves, Landsat, Sundarbans.

Correspondent author E-mail address: dipddm@gmail.com, ORCID ID: https://orcid.org/0000-0002-9889-457X.

Introduction

Forest canopy density is an important biophysical parameter to monitor forest health. It represents the proportion of the sky hemisphere covered by tree crowns when viewed from a single point and is expressed as a percentage of the total area. Roy et al. (1996) developed a three-component crown density model utilising vegetation indices like, Advanced Vegetation Index (AVI), Bare Soil Index (BI) and Shadow Index (SI) for classification of forest crown density. However, ground-based canopy density estimation techniques are time-consuming, labor-intensive and expensive. Therefore, remote sensing approaches have gained prominence. A number of image classification approaches have been successfully applied to estimate FCD from satellite data. This model was developed by Rikimaru et al. (1997) using indices of vegetation, bare soil and shadow and was successfully applied to monitor the health of forests in Indonesia, Thailand and Nepal (Rikimaru, 2002). The FCD Model utilises canopy density as an essential parameter for characterisation of forest conditions. FCD data indicates the degree of degradation, thereby also indicating the intensity of rehabilitation that may be required. The method also makes it possible to monitor transformation of forest conditions over time and assessment of the progress of reforestation activities (Rikimaru et al., 2002). A number of image classification approaches have been successfully applied to estimate FCD from satellite data like visual interpretation, Object-oriented Image Segmentation, Maximum Likelihood Classification (MLC), Linear Regression, FCD Mapper and Artificial Neural Networks (ANN). Nandy et al. (2003) proposed a set of vegetation indices using linear combinations to isolate vegetation cover characteristics which vary with canopy density. Hadi et al. (2004) applied the FCD model to monitor forest degradation and fragmentation in parts of Indonesia and found that the model was unable to differentiate forest canopy among two

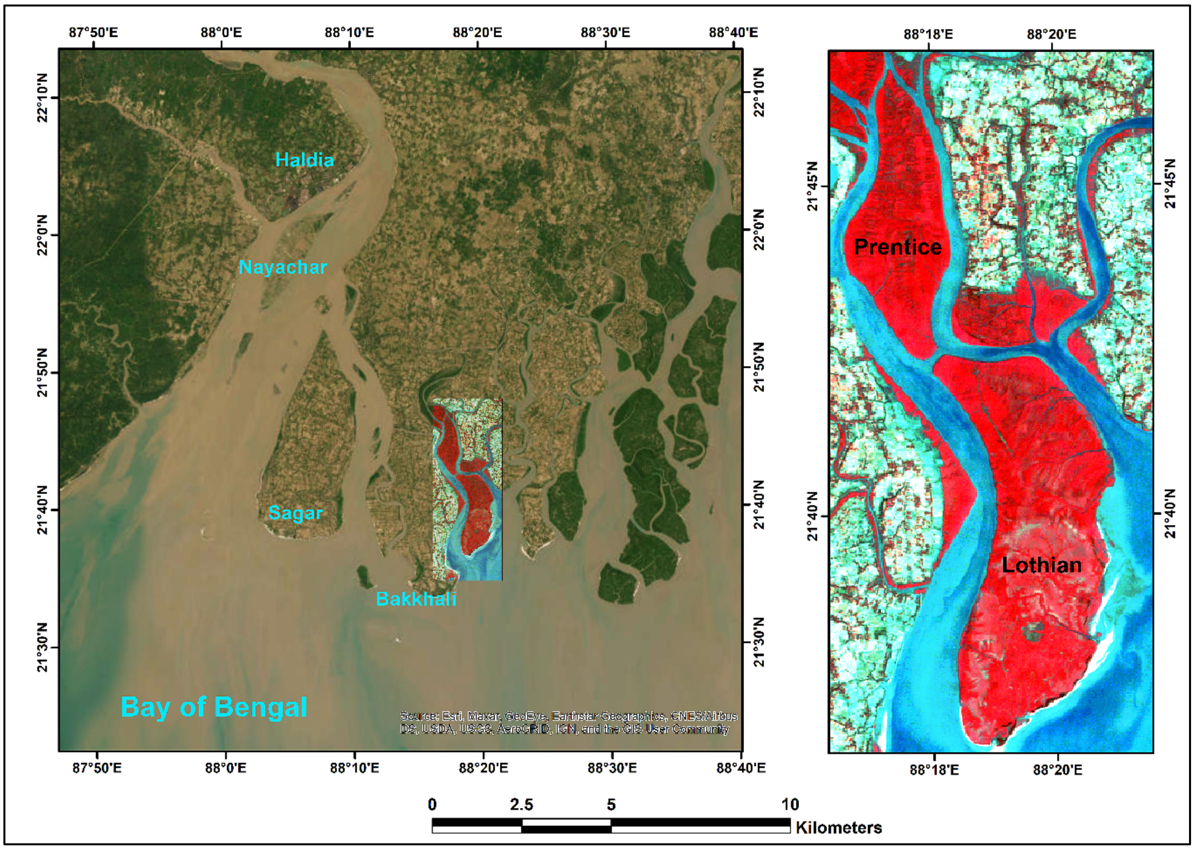

Figure 1a- Location map of the study area.

types of vegetation. In their study, Chandrashekhar et al. (2005) made a comparison of forest canopy density stratification using object-oriented image analysis, conventional method of visual interpretation and FCD Mapper semi expert system. Various authors have attempted to make a comparison of different classification approaches, such as, ANN, Multiple Linear Regression (MLR), Maximum Likelihood Classification (MLC) and Forest Canopy Density (FCD) Mapper (Joshi et al., 2006; Vohland et al., 2007; Panta et al., 2008; Mon et al., 2012). Some attempts have also been made to apply the various spectral indices and classification techniques to monitor the health of the Sundarban mangroves (Giri et al., 2007; Rashid et al., 2009; Majumdar et al., 2012; Rahman et al., 2013).

While the FCD model has been extensively applied to tropical evergreen and deciduous forests, its application to mangrove ecosystems remains unexplored, despite the unique structural and spectral characteristics of mangrove canopies. The May 2009 Aila cyclone had a significant impact on the Prentice and Lothian islands of Indian Sundarban. In order to characterise the types of forest canopy, evaluate the changes in canopy density driven by cyclones, and offer potential causes for these changes, the forest canopy density (FCD) has been calculated for both islands in the present study.

Study area

The Sundarban is an archipelago of several hundred islands, spread across 9,630 km^2 in India and 16,370 km^2 in Bangladesh. The forest lies on the delta of the Ganga, Brahmaputra and Meghna Rivers on the northern part of Bay of Bengal. It is home to the world's largest mangrove forest. The Sundarban supports an exceptional biodiversity with a wide range of flora and fauna, including more than 27 mangrove species, 40 species of mammals, 35 species of reptiles, and 260 bird species. The area is primarily composed of a complex network of tidal channels, mudflats, and mangrove forests. The Prentice and Lothian islands are a part of the Namkhana block of South 24 Parganas. Lying between $21^\circ 36' $ N to $21^\circ 46'$ N and $88^\circ 16'$ E to $88^\circ 20'$ E the Prentice and Lothian group of islands covers a total area of 51.59 km^2 (Figure 1)

The region experiences a tropical monsoon type of climate, with summer temperatures ranging from 28°C to 35°C and winter temperatures ranging from 10°C to 25°C. Rainfall in the area varies between 1500 mm to 2800 mm, occurring mostly during the monsoon season lasting from June to October. Cyclonic activities, tidal surges, and coastal erosion are quite common throughout the Sundarban region.

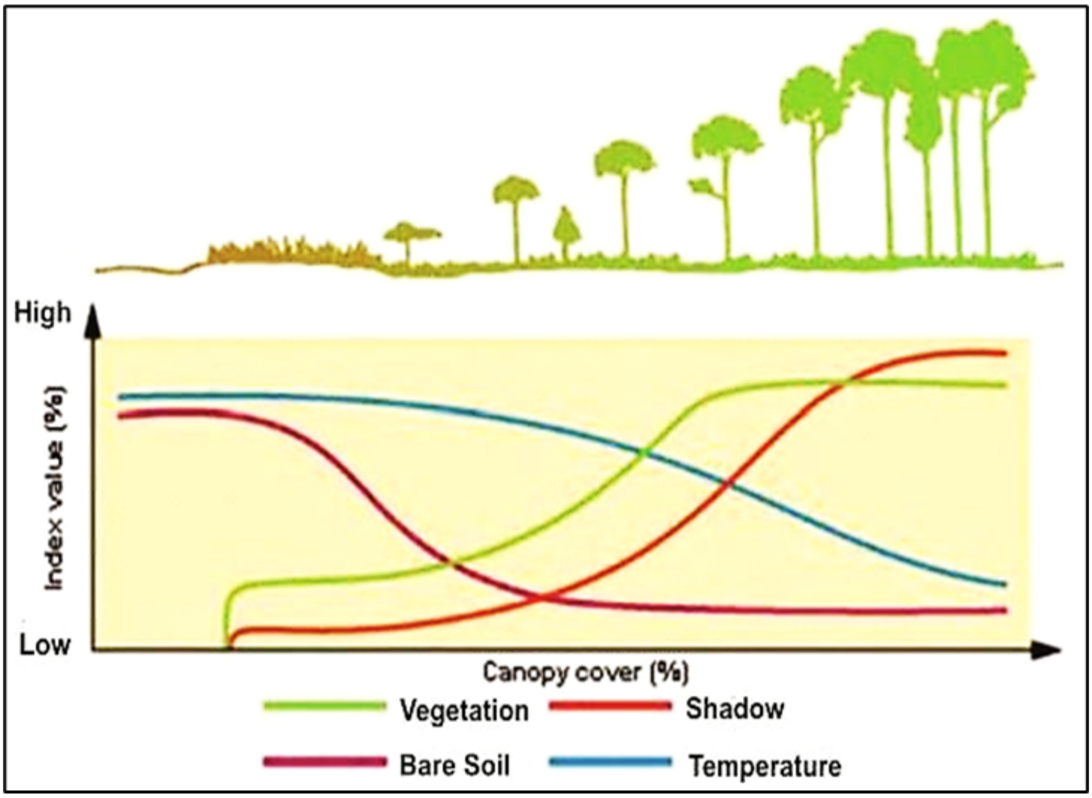

Figure 1b- The characteristics of the four indices for forest condition (Rikimaru et al. 2022).

The Prentice and Lothian islands are situated in the Saptamukhi estuary, about 10 to 12 km eastward of the Hugli estuary. These low, marshy islands are still in the process of formation through the action of tidal currents and siltation. The roots of these plants trap sediments from tidal waters and are instrumental in growth of the islands through the process of bio-tidal accretion. Common mangrove species found in this region are Avicenia, Xylocarpus, Sonneratia, Bruguiera, Rhizophora etc. With time as the land is raised above the high tide level, mangrove succession advances towards terrestrial plants which are less salt tolerant and cannot endure long term inundation. Mangrove forests exhibit distinct zonation patterns driven primarily by local geomorphology and soil salinity gradients associated with tidal inundation frequency, resulting in characteristic variations in canopy density.

Severe Cyclonic Storm Aila, which formed over the Bay of Bengal, made landfall on May 25, 2009, with sustained wind speeds of 110 km/h. Aila became the most devastating cyclone the Sundarban region witnessed since Cyclone Sidr in 2007. The landfall time of the cyclone closely coincided with new moon conditions, and as a result tidal effects were amplified and produced 3.3 meters storm surge above predicted levels at Sagar Island. Maximum areas of Sundarban mangrove forest were inundated with up to 6.1 meters of water, and the areas remained under 2.4 meters of water for an extended periods post-cyclone. The long-term inundation caused wider spread damage to the mangrove forest and altered soil chemistry through widespread saltwater intrusion. About 3.9 million people in the area were impacted by the cyclone, which also severely damaged 778 km of protective embankments and 4,000 km^2 of mangrove forests. Cyclone Aila is the perfect case study for evaluating mangrove forest resilience and recovery patterns using remote sensing techniques because of the extended exposure to saltwater, which not only resulted in immediate vegetation mortality but also caused changes in mangrove succession patterns that lasted for years.

Methodology

In the present study, Landsat 5 TM data of 2009 (pre-Aila) and 2010 (post-Aila) were acquired for assessing the cyclone impact on forest canopy density. The images were geometrically corrected through the process of image-to-image registration where a second-degree polynomial was applied to achieve the acceptable root mean square error (RMSE < 0.5 pixels). Radiometric and atmospheric correction was performed for both the images using the standard 6S method of Chander et al, (2009).

The correction process involved two sequential steps: conversion to at-sensor spectral radiance and subsequent transformation to top-of-atmosphere (TOA) reflectance. The first step converts image data from multiple sensors and platforms into a physically meaningful common radiometric scale whereas the TOA reflectance was calculated to remove the effects of solar zenith angle variations, differences in exo-atmospheric solar irradiance, and Earth-Sun distance variations.

The radiometrically and atmospherically corrected images were then processed to obtain the Forest Canopy Density. The Forest Canopy Density Model (FCD) combines biophysical and spectral characteristics using four complementary indices, namely, Advanced Vegetation Index (AVI), Bare Soil Index (BI), Shadow Index (SI) and Thermal Index (TI) that respond differently to forest structural properties. AVI has a positive relationship with the quantity of vegetation (Figure 2). Thus, its value is high for high forest density and low for low forest density and bare land. Since BI is a function of the amount of bare soil, it increases when ground exposure increases and forest density decreases (Rikimaru et al., 2002). The SI value rises in tandem with an increase in the FCD value. Put in another context, there is greater shade where there is more vegetation growth. Due to the cooling effect of leaf evaporation and the blockage and absorption of solar radiation, TI has a negative correlation with forest density (Baynes, 2004).

Table 1- Spectral indices calculated to support the FCD model output.

INDEX	FORMULA	REFERENCE
NORMALIZED DIFFERENCE VEGETATION INDEX (NDVI)	NDVI = (NIR – RED)/(NIR + RED)	Rouse, 1974
ADVANCED NORMALIZED VEGETATION INDEX (ANVI)	Derived from AVI and NDVI by principal component analysis (First component).	Su Mon, 2012
SOIL ADJUSTED VEGETATION INDEX (SAVI)	SAVI= (NIR – RED/NIR + RED + L)* (1 + L)	Huete, 1988
PERPENDICULAR VEGETATION INDEX (PVI)	PVI = sin(a) NIR - cos(a) RED	Richardson and Wiegand (1977)
COMBINED SPECTRAL RESPONSE INDEX (COSRI)	COSRI= [(BLUE + GREEN)/(RED + NIR)]* NDVI	Fernandez, 2006
SPECIFIC LEAF AREA INDEX (SLAI)	SLAI= NIR/(RED – MIR2)	Fernandez, 2006
NORMALIZED DIFFERENCE WATER INDEX (NDWI)	NDWI= (GREEN – NIR)/(GREEN + NIR)	Gao, 1996

Spectral Index Calculation

Advanced Vegetation Index (AVI): AVI is modified form of NDVI. It examines the status of chlorophyll-a in the leaf segment by suppressing the RED reflectance and enhancing the NIR reflectance.

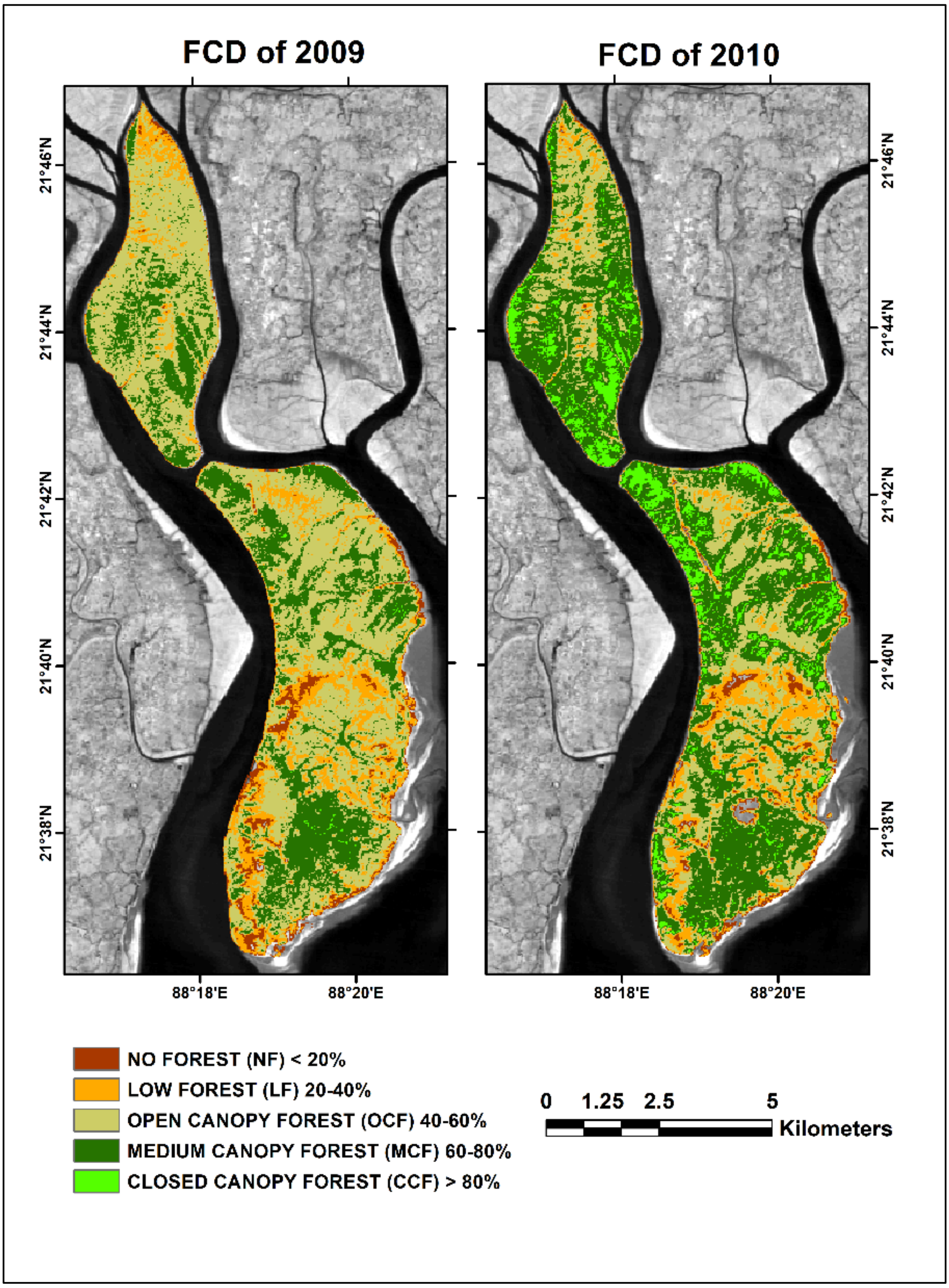

Figure 2- Forest Canopy Density (FCD) of Prentice and Lothian Islands respectively for 2009 (pre-Aila) and 2010 (post-Aila).

AVI = [NIR × (256 – RED) × (NIR – RED) + 1]1/3, when (NIR – RED) > 0 (Eq. -1)

Table 1- Correlations among calculated spectral indices.

YEAR	2009		2010	
VARIABLES	**LINEAR EQUATION**	**(r^2)**	**LINEAR EQUATION**	**(r^2)**
AVI - FCD	0.93195*AVI - 2.41751	0.971	0.9976*AVI - 2.96219	0.872
BI - FCD	-0.64577*BI – 0.38649	0.534	-0.48797*BI – 0.22555	0.687
SSI - FCD	0.94423*SSI + 0.0021	0.971	1.0234*SSI + 0.00098	0.872
VD - FCD	0.98716*VD + 0.03173	0.954	0.79917*VD + 0.0913	0.921
NDVI - FCD	3.92042*NDVI - 0.76964	0.970	3.0724*NDVI - 0.99165	0.899
ANVI - FCD	1.06251*ANVI + 0.00391	0.972	1.17701*ANVI - 0.00251	0.884
SAVI - FCD	6.32228*SAVI - 0.6741	0.974	5.34421*SAVI - 0.89987	0.918
SLAI - FCD	1.0882*SLAI - 0.89009	0.684	0.31107*SLAI - 0.02174	0.462
COSRI - FCD	5.09513*COSRI - 1.04342	0.911	5.22287*COSRI - 1.35477	0.655
NDWI - FCD	-4.55506*NDWI – 0.45277	0.902	-3.8331*NDWI – 0,9058	0.845

Bare Soil Index (BI): Fore more reliable estimation of the vegetation status Bare Soil Index (BI) is formulated with medium infrared information. By combining both vegetation and bare soil indices in the analysis, one may assess the status of forest lands on a continuum ranging from high vegetation conditions to exposed soil conditions. The formula for BI is as follows:

BI = [(MIR + RED) - (BLUE + NIR)/ (MIR + RED) + (BLUE + RED)] 1/3 (Eq. -2)

Shadow Index (SI): One unique characteristic of a forest is its three dimensional structure to extract information on the forest structure from satellite data, the new methods examine the characteristics of shadow by utilising spectral information on the forest shadow itself and thermal information on the forest influenced by shadow. The shadow index is formulated through extraction of the low radiance of visible bands.

SI = ((256-BLUE) * (256-GREEN) * (256-RED)) 1/3 (Eq. -3)

Scaled Shadow Index (SSI): Since the values of shadow index are relative and vary with different illumination condition, SI was normalised to Scaled Shadow Index (SSI) through Principal Component Analysis (PCA). SSI enables differentiation between vegetation in the canopy and ground-level vegetation, significantly improving the assessment forest structure.

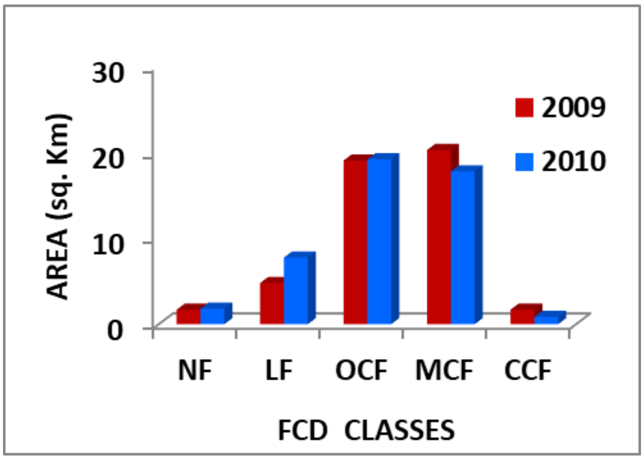

Figure 3- Changes in the total area of the canopy density classes.

Vegetation Density (VD): It is the procedure to synthesise AVI and BI using PCA. The first principal component (PC1) is taken as VD due to its maximum shared variance. This is done essentially because AVI and BI have high negative correlation.

Forest Canopy Density (FCD): The final FCD was calculated by integrating VD and SSI using the following transformation:

$$FCD = (VD * SSI+1)1/2 -1 \qquad \text{(Eq. -4)}$$

This integration produces FCD values as percentages, representing forest canopy density on a continuous scale from 0% (no forest) to 100% (closed canopy forest). FCD values were classified into five ecologically meaningful categories based on histogram analysis and mangrove ecology principles:

1. No Forest (NF): 0-5% density
2. Low Forest (LF): 5-40% density
3. Canopy Forest (OCF): 40-60% density
4. Medium Canopy Forest (MCF): 60-80% density
5. Closed Canopy Forest (CCF): 80-100% density

FCD was calculated separately for both 2009 and 2010 respectively. Thereafter, A comprehensive change detection matrix was developed using class combination analysis to identify pixel-to-pixel transitions between pre-Aila and post-Aila conditions. The matrix quantified all possible transitions between the five FCD classes, enabling detailed assessment

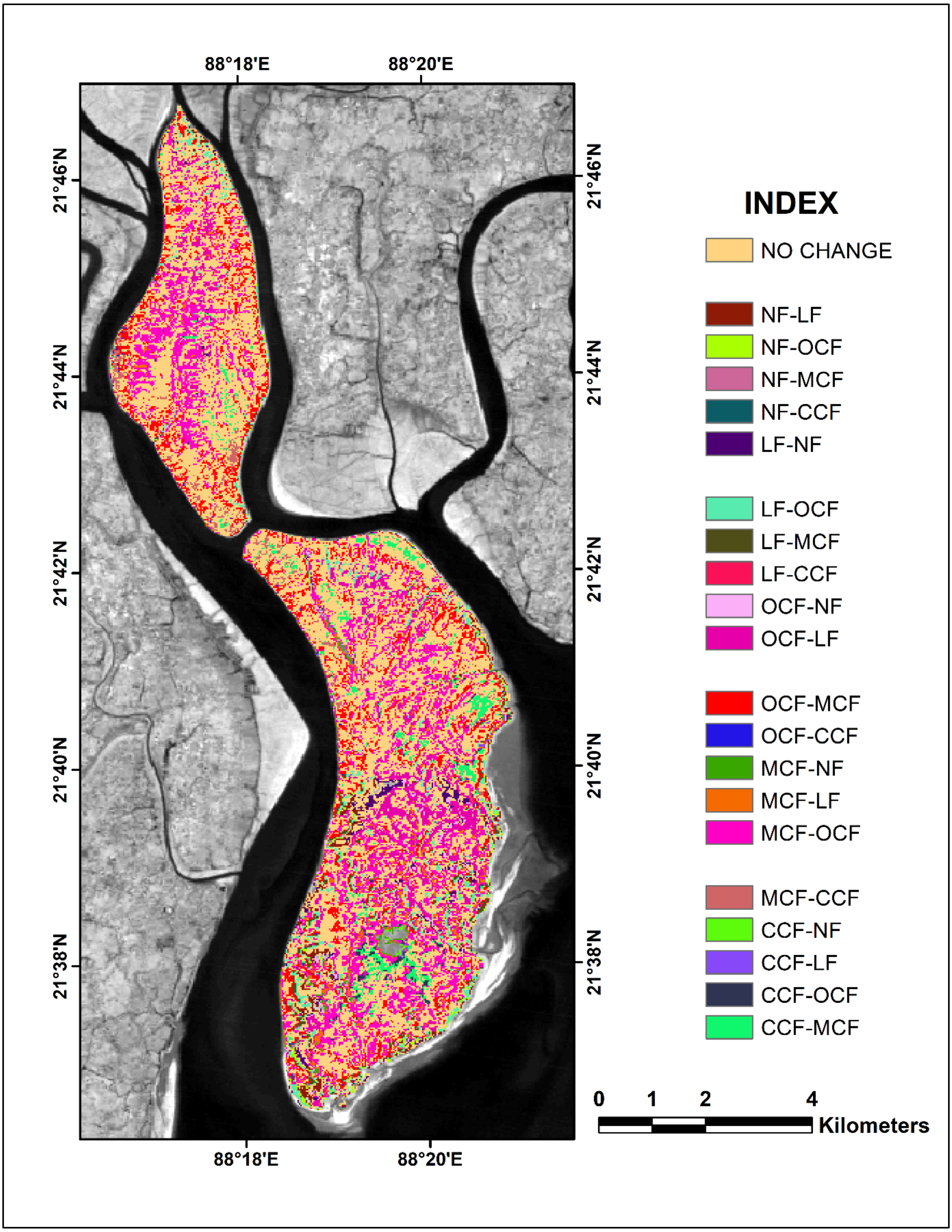

Figure 4- Pixel to pixel changes in Forest Canopy Density between 2009 and 2010 using the combination analysis.

of Canopy degradation, Canopy regeneration and No-change areas respectively. Finally, multiple complementary vegetation indices such as, NDVI, ANVI, SAVI, SLAI, PVI, COSRI AND NDWI were also calculated to validate the FCD Model output (Table 1). Linear correlation analysis was performed between these indices and FCD to assess model consistency and reliability.

Results and Discussion

The AVI for 2009 ranged from 0.59 to 3.61 whereas in 2010 it increased to 0.34 to 4.17. The wider range in 2010 indicates increased geographic diversity in vegetation response, with certain regions exhibiting total vegetation loss (lower minimum values) while others indicated increased vegetative vigour (higher maximum values). BI indicates the degree of exposure of bare ground surface and shows an increase from 1.78 to 0.04 (2009) to -2.45 to 0.32 (2010). The extent of bare surface had increased in 2010 around previously existing bare surface and also in previously vegetated northern parts of Lothian Island. SI had relatively narrow ranges in both years (0.801–0.879 in 2009 and 0.747–0.922 in 2010). The wider range in 2010 was due to changes in the complexity of the canopy structure. The lower minimum values in 2010 correspond to areas where canopy loss reduced shadow patterns. The higher maximum values are for places where the remaining vegetation made shadow effects more pronounced because of the higher structural contrast.

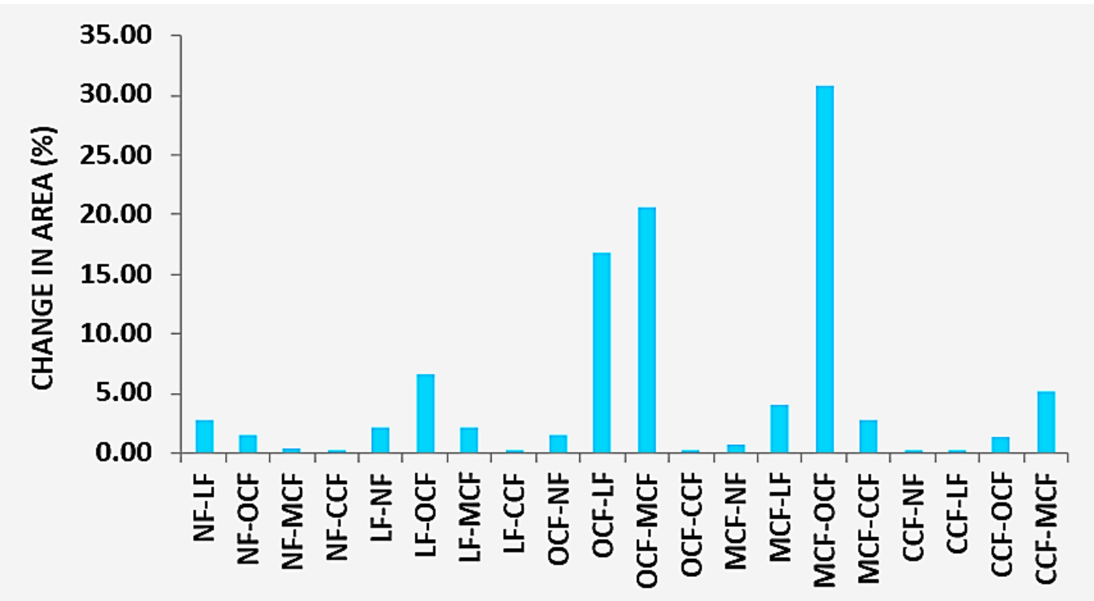

Figure 5- Bar graph showing change detection results of FCD.

PCA between AVI and BI provided strongly successful dimension reduction, with PC1 accounting for 75.62% variance in 2009 and 86.11% in 2010. The higher explained variance in 2010 implies greater correlation between vegetation cover and soil exposure post-cyclone. The VD offers a continuous range of vegetation from dense vegetation to bare land. In case of

Prentice Island, the VD has increased between 2009 and 2010 along the southern edge of island, whereas the interior portion has remained unaltered. However, VD shows an overall decline throughout the Lothian Island, the decline being specially marked in the south eastern portion of the island. SSI validates the strong relationship between vegetation vigour and shadow patterns in mangrove canopies. The first principal component (PC1), which explains more than 99% of the variance in AVI and SI, is extracted as the SSI. It shows a slight decline in the central portion of Prentice Island and the southeastern portion of Lothian Island.

The FCD was obtained by integrating the two end members, namely, VD and SSI of each year respectively. The FCD for each year was divided into five classes from the histogram of each raster, like, No Forest (NF), Low Forest (LF), Open Canopy Forest (OCF), Medium Canopy Forest (MCF) and Closed Canopy Forest (CCF) (Figure 3). It is observed that between 2009 and 2010 the overall area under NF and LF has increased whereas, the total area under MCF and CCF has decreased. However, the total area under OCF has shown no change within this time period (Figure 4). Several other vegetation indices are calculated to validate the output of the FCD Model (Table 2).

Table 2- Change detection matrix showing the changes in area (Sq. Km) between 2009 and 2010 under different FCD classes.

Class	NF	LF	OCF	MCF	CCF
NF	0.358	0.618	0.333	0.103	0.004
LF	0.479	2.085	1.456	0.478	0.014
OCF	0.322	3.762	9.970	4.594	0.062
MCF	0.163	0.909	6.865	11.392	0.609
CCF	0.031	0.056	0.292	1.139	0.161

Correlation analysis between FCD and related vegetation indices demonstrated strong relationships for both years. The highest correlation was found between NDVI ($r^2 = 0.970$ in 2009; $r^2 = 0.899$ in 2010) and FCD, followed by SAVI ($r^2 = 0.974$ in 2009; $r^2 = 0.918$ in 2010) and ANVI ($r^2 = 0.972$ in 2009; $r^2 = 0.884$ in 2010). The consistently high correlations validate the effectiveness of the FCD model in capturing vegetation density variations. NDWI exhibited negative correlations ($r^2 = 0.902$ in 2009; $r^2 = 0.845$ in 2010), proving the anticipated inverse relationship between water presence and forest canopy density (Table 2).

A one-way ANOVA test was performed between FCD 2009 and FCD 2010 to identify the mean difference. It is a preparatory step for any type of change detection study because without significant differences the change detection study cannot be meaningful. The pre and post-cyclone FCD distributions were found to exhibit highly significant differences ($F = 4568.62$, $p < 0.001$), as confirmed by the one-way ANOVA analysis. The observed changes are a result of legitimate cyclone-induced modifications, as the between-group variation (93.454) was significantly greater than the within-group variation (0.021). This suggests that the observed changes are not the result of natural variability or measurement error. Thereafter a change detection matrix was developed using class combination analysis to show the pixel to pixel change between FCD 2009 and FCD 2010 (Figure 5). Table 3 shows the total changes in area under each of the five canopy classes between 2009 and 2010. It is found that within each class maximum portion of the area has remained unchanged.

Replacement of one community of species with another is a natural phenomenon in mangrove succession, but the abnormal changes in the pattern indicate the influence of some threshold event like the Aila cyclone (Figure 5 & Table 3). The degeneration of canopy cover due to the prevalence of unhealthy conditions is reflected in the negative class migrations, i.e., the shift from higher canopy density to lower canopy density (Table 3). Since 30.79% (Figure 6) of Medium Canopy Forest (MNF) was converted to Open Canopy Forest (OCF) in 2010, MNF has seen the most degradation. Figure 6 shows that 16.87% of open canopy forest has degraded to Low Forest (LF) and around 5.11% of closed canopy forest (CCF) has degraded to medium canopy forest (MNF). As a result, canopy degradation has affected an area of 14.03 km^2. This degradation occurred mainly in the interiors of the islands, where cyclone-induced storm surge has caused long-term inundation and the formation of hypersaline tracts, which retards the growth of higher-order mangroves (Figure 5 & 6). However, positive class migrations from Open Canopy Forest (OCF) to Medium Canopy Forest (MCF) (20.60%) and Low Forest (LF) to Open Canopy Forest (OCF) (6.53%) (Figure 6) show that the canopy has recovered around the islands' periphery following the storm. Initially the canopy in these areas too was destroyed, but the cyclone-induced sedimentation along the banks of the islands has created a new setup for the development of neo-mangroves (Figure 5 & 6). These are associated with low canopy density and indicate the initiation of the first stages of mangrove succession.

Overall assessment depicts that the species in Open Canopy Forest (OCF) such as, Acanthus Ilicifolius, Nypa Fruticans, Crinium Defixum, Cryptocoryne Ciliate etc. are better able to adapt with the changed conditions because even though they have suffered damage their overall area has remained unchanged between 2009 and 2010. Medium and Closed Canopy Forest areas, characterised by mature Avicennia, Rhizophora, and Bruguiera species,

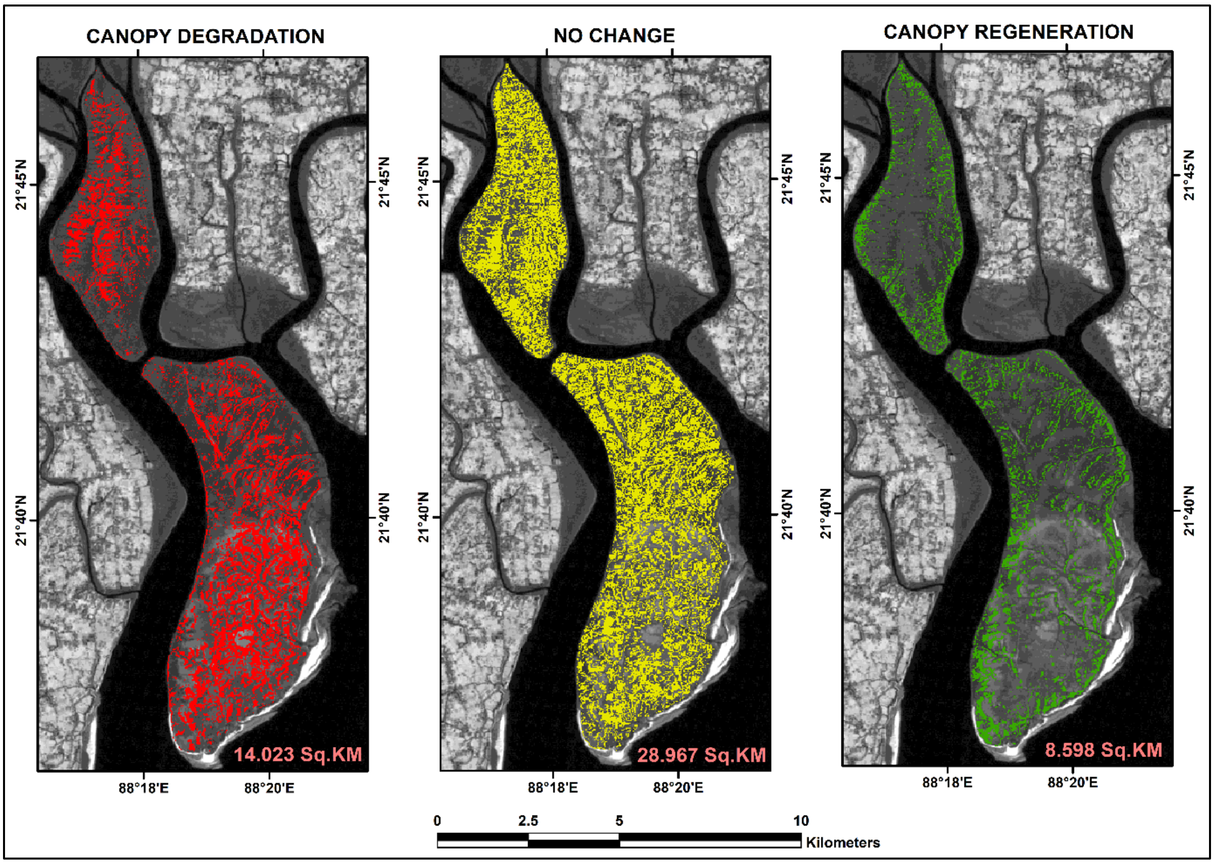

Figure 6- Spatial patterns of canopy degradation and regeneration.

experienced the most severe degradation. The significant mortality and damages to mature mangrove stands caused by the 30.79% shift from MCF to OCF is probably due to the combined impacts of mechanical wind damage, prolonged flooding, and hypersaline conditions (Giri et al., 2007; Majumdar et al., 2012).

Spatial degradation and regeneration patterns have distinct correlations with geomorphology at the local scale. The interior island zones, which were subjected to extended flooding and poor drainage, registered focused patterns of degradation (Figure 7). These areas developed hypersaline conditions due to evaporation of trapped seawater, creating hostile environments for mangrove survival. In contrast, regeneration patterns were most focused on island peripheries where cyclone-induced sedimentation had provided favourable environments for mangrove colonisation (Figure 7). Deposition of new sediment along island rim had offered effective substrates for pioneering mangrove species colonisation, initiating new successional sequences (Rashid et al., 2009; Majumdar et al., 2012; Rahman et al., 2013). The recorded changes are a fundamental perturbation to established patterns of mangrove succession. Classic succession theory predicts slow, progressive transitions from pioneer to climax species communities within decadal timescales. Cyclone Aila condensed these transitions into a single disturbance episode, producing a complex mosaic of successional stages. The concurrent occurrence of regeneration and degradation processes at various geographical scales illustrates how cyclone impacts on mangrove ecosystems are not consistent. Some regions started new successional sequences that might eventually improve ecosystem resilience, whereas others suffered decades-long setbacks in successional development.

Conclusion

The Aila cyclone has significantly affected the forest canopy density of Prentice and Lothian islands, bringing about changes in the pattern of mangrove succession. The process of canopy degradation and regeneration is linked with the geomorphology of the region. Strong cyclonic winds and long-term inundation have damaged canopy density in 14.03 km^2 of the total area. The recorded response patterns provide significant information on mangrove ecosystem dynamics under severe weather conditions anticipated to increase with global climate change. The 1.63:1 degradation-to-regeneration ratio implies that individual extreme events can lead to net ecosystem losses, with long-term implications for the persistence of mangrove forests under increasing cyclone frequency and intensity. However, in much of the area canopy cover has regenerated indicating that the mangroves are adjusting with the changed hydro-geomorphological conditions and moving towards a state of dynamic equilibrium.

In mangrove evaluation, where conventional classification techniques frequently fall short of capturing the structural complexity of mixed species stands, the capacity of the FCD model to identify minute changes in canopy density proved very useful. Thus, the FCD model, which earlier has been applied only in case of tropical evergreen and deciduous forests, is also useful for assessment of mangrove forests. Such type of technique and modelling is helpful in evaluation of forest cover where direct field investigation is not feasible. These findings underline the necessity for adaptive management techniques that acknowledge the resilience and susceptibility of mangrove ecosystems under varying climatic circumstances, which have substantial implications for coastal zone management and climate adaptation plans.

Acknowledgements

The author acknowledges the infrastructural support provided by the Department of Remote

Sensing and GIS, Vidyasagar University, and the Department of Geology, University of Calcutta. Special gratitude is extended to the officials at Microimages (TNT Mips) for their valuable assistance in this research. The author also wishes to thank Atrayee Biswas from the Department of Geography, The Bhawanipur Education Society College, for her contributions to this work.

References:

Baynes, J. (2004): Assessing forest canopy density in a highly variable landscape using Landsat data and FCD Mapper software, *Australian Forestry*, 67. 247–253.

Chander, G., Markham, B.L., Helder, D.L. (2009): Summary of current radiometric calibration coefficients for Landsat MSS, TM, ETM+, and EO-1 ALI sensors, *Remote Sensing of Environment*, 113. 893–903.

Chandrashekhar, M.B., Saran, S., Raju, P. L. N., and Roy, P. S. (2005): Forest Canopy Density Stratification: How Relevant is Biophysical Spectral Response Modelling Approach? *Geocarto International,* 20(1). 15-21.

Fernandez-Buces, N., Siebe, C., Cram, S. (2006). Mapping soil salinity using a combined spectral response index for bare soil and vegetation: a case study in the former lake Texcoco, Mexico. *Journal of Arid Environments*, 65(4). 644–667.

Giri, C., Pengra, B., Zhu, Z., Singh, A., and Tieszen, L.L. (2007): Monitoring mangrove forest dynamics of the Sundarbans in Bangladesh and India using multi-temporal satellite data from 1973 to 2000, *Estuarine, Coastal and Shelf Science*, 73. 91-100.

Hadi, F., Wikantika, K., and Sumarto, I. (2004): Implementation of Forest Canopy Density Model to monitor forest fragmentation in Mt. Simpang and Mt. Tilu Nature Reserves, West Java, Indonesia, *3rd FIG Regional Conference*, Jakarta, Indonesia, October 3-7, 2004.

Huete, A. R., (1988): A Soil-Adjusted Vegetation Index (SAVI), *Remote Sensing of Environment*, 25. 295-309.

Joshi, C., Leeuw, J.D., Skidmore, A.K., Duren, I.C.V., and Oosten, H.V. (2006): Remotely sensed estimation of forest canopy density: a comparison of the performance of four methods, *International Journal of Applied Earth Observation and Geoinformation*, 8. 84–95.

Majumdar, D.D., Bera, S., Ray, R., and Paul, A.K., (2012). An assessment of diversities in halophytic grassland and mangrove swamp in Nayachar Island, Hugli estuary, West Bengal. Some aspects of coastal vegetation in India, including Andamans and Sundarbans. Ramnagar College, Depal, 112–123.

McFeeters, S.K. (1996): The use of Normalized Difference Water Index (NDWI) in the delineation of open water features, *International Journal of Remote Sensing*, 17(7). 1425–1432.

Nandy, S., Joshi, P.K., and Das, K.K. (2003): Forest canopy density stratification using biophysical modelling. *Journal of the Indian Society of Remote Sensing,* 31. 291–297.

Panta, M., Kim, K., and Joshi, C. (2008): Temporal mapping of deforestation and forest degradation in Nepal: Applications to forest conservation, *Forest Ecology and Management*, 256. 1587–1595.

Rahman, M.M., Ullah, M.R., Lan, M., Sri Sumantyo, J.T., Kuze, H., and Tateishi, R. (2013): Comparison of Landsat image classification methods for detecting mangrove forests in Sundarbans, *International Journal of Remote Sensing*, 34(4). 1041-1056.

Rashid, S.H., Biswas, S.R., Bocker, R., and Kruse, M. (2009): Mangrove community recovery potential after catastrophic disturbances in Bangladesh, *Forest Ecology and Management*, 257. 923–930.

Richardson, A. J., and Wiegand, C. L. (1977): Distinguishing vegetation from soil background information, *Photogrammetric Engineering and Remote Sensing*, 43. 1541-1552.

Rikimaru, A., and Miyatake, S. (1997): Development of forest canopy density mapping and monitoring model using indices of vegetation, bare soil and shadow. In *18th Asian Conference on Remote Sensing*, 20–24 October, Malaysia.

Rikimaru, R., Roy, P.S., and Miyatake, S. (2002): Tropical forest cover density mapping, *Tropical Ecology*, 43. 39–47.

Rouse, J. W., Haas, R. H., Schell, J. A., Deering, D. W., and Harlan, J. C. (1974): Monitoring the vernal advancement and retrogradation (greenwave effect) of natural vegetation, NASA/GSFC Type III Final Report, Greenbelt, Md. 371.

Roy, P.S., Sharma, K.P., and Jain, A. (1996): Stratification of density in dry deciduous forest using satellite remote sensing digital data – an approach based on spectral indices, *Journal of Biosciences*, 21. 723–734.

Su Mon, M., Mizoue, N., Htun, N.Z., Kajisa, T., and Yoshida, Y. (2012): Estimating forest canopy density of tropical mixed deciduous vegetation using Landsat data: A comparison of three classification approaches, *International Journal of Remote Sensing*, 33(4). 1042-1057.

Vohland, M., Stoffels, J., Hau, C., and Schüler, G. (2007): Remote sensing techniques for forest parameter assessment: multispectral classification and linear spectral mixture analysis, *Silva Fennica,* 41(3). 441–456.